Calcium Buffering and Excitation-Contraction Coupling in Developing Avian Myocardium

Tony L. Creazzo,* Jarrett Burch,* and Robert E. Godt†
*Neonatal/Perinatal Research Institute, Department of Pediatrics/Neonatology Division, Duke University Medical Center, Durham, North Carolina; and †Department of Physiology, Medical College of Georgia, Augusta, Georgia

ABSTRACT This report provides a detailed analysis of developmental changes in cytoplasmic free calcium (Ca^{2+}) buffering and excitation-contraction coupling in embryonic chick ventricular myocytes. The peak magnitude of field-stimulated Ca^{2+} transients declined by 41% between embryonic day (ED) 5 and 15, with most of the decline occurring between ED5 and 11. This was due primarily to a decrease in Ca^{2+} currents. Sarcoplasmic reticulum (SR) Ca^{2+} content increased 14-fold from ED5 to 15. Ca^{2+} transients in voltage-clamped myocytes after blockade of SR function permitted computation of the fast Ca buffer power of the cytosol as expressed as generalized values of B_{max} and K_D. B_{max} rose with development whereas K_D did not change significantly. The computed SR Ca^{2+} contribution to the Ca^{2+} transient and gain factor for Ca^{2+}-induced Ca^{2+} release increased markedly between ED5 and 11 and slightly thereafter. These results paralleled the maturation of SR and peripheral couplings reported by others and demonstrated a strong relationship between structure and function in development of excitation-contraction coupling. Modeling of buffer power from estimates of the major cytosolic Ca binding moieties yielded a B_{max} and K_D in reasonable agreement with experiment. From ED5 to 15, troponin C was the major Ca^{2+} binding moiety, followed by SR and calmodulin.

INTRODUCTION

Contraction of the myocardium is initiated by depolarization of the membrane, followed by net entry of Ca^{2+} through voltage-gated Ca^{2+} channels. In the adult heart, this Ca^{2+} causes a further release of Ca^{2+} from the sarcoplasmic reticulum (SR) via a mechanism termed Ca^{2+}-induced Ca^{2+} release (CICR). The subsequent rise in intracellular Ca^{2+} causes cyclic interactions between the contractile proteins myosin and actin, which give rise to force production and shortening of the muscle cell. Relaxation of the cell is caused primarily by a decrease in the intracellular level of Ca^{2+} due to active uptake of Ca^{2+} back into the SR and extrusion via Na^+/Ca^{2+} exchange. The processes linking depolarization of the membrane and the ensuing rise and fall in intracellular Ca^{2+} is termed excitation-contraction (EC) coupling (reviewed in Bers, 2001).

In mammals, it is often considered that SR content is sparse at birth and undergoes most of its development postnatally (Nakanishi and Jarmakani, 1984). This appears to be true in rabbit and rat hearts (Seguchi et al., 1986a; Nakanishi et al., 1992) but not true for guinea pigs, which have a fully developed SR at birth (Goldstein and Traeger, 1985). Thus, there is variation among mammalian species with respect to the degree of maturity of SR at birth. In the chick, SR morphology and function is well developed by hatching. Presumably because of technical difficulties, there are currently no published reports of detailed analysis of SR function and CICR in mammalian embryonic heart development.

The chick heart has long been the standard for the study of developmental physiology and morphology and remains the best described of any vertebrate model of development. The normal physiology of the developing chick heart has long been characterized (Sperelakis, 1982) and there is information available on altered cardiac function in a chick model of human heart disease (Creazzo et al., 1998). Moreover, a comprehensive study of the morphology of the formation and maturation of SR junctional complexes is available only for the chick embryo (Protasi et al., 1996).

CICR in chick develops early and is present well before hatching, probably by embryonic day (ED) 4–5, as ryanodine receptors are first detected at about this time (Dutro et al., 1993). The chick heart begins beating at ~ED1.5 (Sperelakis, 1982). As the myocardium develops, SR and contractile proteins proliferate and myofibrils are formed. After ED5, the myofibrils are abundant and are aligned parallel to one another in the cell (Manasek, 1970). As the content of myofibrils increases, the force of contraction increases apace (Godt et al., 1991). In the early chick heart, relaxation is caused primarily by removal of Ca^{2+} from the cell by Na^+/Ca^{2+} exchange proteins in the sarcolemma. With development, the SR begins to play a larger role in control of intracellular Ca^{2+}, such that from around the time of hatching (ED22) and beyond, Na^+/Ca^{2+} exchange is subsidiary to the SR (Vetter et al., 1986).

Recently, the elegant work of Franzini-Armstrong, Protasi, and colleagues has provided detailed information on the development of SR-plasma membrane junctional complexes involved in EC coupling in the chick heart (Sun et al., 1995; Protasi et al., 1996). In these studies, complete junctional

Submitted February 13, 2003, and accepted for publication September 23, 2003.

Address reprint requests to Tony L. Creazzo, PhD, Neonatal/Perinatal Research Institute, Pediatrics/Neonatology Division, Duke University Medical Center, DUMC Box 3179, Durham, NC 27710. Tel.: 919-681-8422; Fax: 919-668-1599; E-mail: tcreazzo@duke.edu.

0006-3495/04/01/966/12 $2.00

complexes are described as having a junctional gap, which is fully zippered by closely spaced feet (RyRs). Dihydropyridine receptors (DHPRs) are clustered in the plasma membrane in close proximity to the RyRs at junctional complexes but as in adult hearts, lack the ordered arrays seen in skeletal muscle. The junctions are confined to the peripheral surface membrane as avian heart, like mammalian embryonic heart, lacks t-tubules, and extended junctional SR and corbular SR do not begin to appear until after hatching (Jewett et al., 1973; Sommer, 1995; Junker et al., 1994). Complete junctions or peripheral couplings are essentially absent at ED4 but increase rapidly and are nearly at the adult level by ED11. From these earlier findings, it is expected that both the efficiency or gain factor for CICR and the overall SR contribution to the Ca^{2+} transient will increase with development, and parallel the development of SR junctional complexes.

An important factor in considering the development of Ca^{2+} handling mechanisms in cardiac muscle is the concomitant developmental change in the rapid Ca^{2+} buffering capacity of the cytoplasm. In adult myocardium, cytoplasmic buffering capacity is quite robust. For every 80–100 Ca^{2+} entering during an action potential, only one Ca^{2+} can be detected with a fluorescent indicator. The rest are bound by rapid Ca^{2+} binding moieties in the cytoplasm (Berlin et al., 1994). The more prevalent Ca^{2+} binding moieties include troponin C (TnC), the SR, and negatively charged membranous structures (Bers, 2001). These and other Ca^{2+} binding moieties are expected to increase with development as the contractile elements increase and become more compact and the myocytes mature. Therefore the impact of ''fast'' Ca^{2+} buffers on cytosolic Ca^{2+} transients is expected to increase with development.

In this report we find that Ca^{2+} transients and Ca^{2+} currents decrease whereas the SR Ca^{2+} content and the Ca^{2+} binding capacity of fast Ca^{2+} buffers in the cytosol increases with development. Whereas TnC binds >50% of the entering Ca^{2+} throughout development, the proportion of Ca^{2+} bound by various other moieties during a Ca^{2+} transient change with development and largely reflects the increasing SR component. The Ca^{2+} buffering capacity (expressed as B_{max} and K_D) along with physiological measurements are used to calculate a gain factor for CICR. As expected, the gain increases with development. The relative increase in SR, as indicated by the increase in gain, paralleled closely the morphological maturation of SR/sarcolemmal junctional complexes previously reported in the elegant study by Protasi et al. (1996; see their Fig. 4). Our results indicate a strong relationship between structure and function in the development of cardiac EC coupling.

METHODS

Myocyte preparation

The culture method used in this study was as originally established by R. L. DeHaan ~20 years ago specifically for the study of Ca^{2+} and Na^{+} currents in chick heart development (personal communication; Kawano and DeHaan, 1991; Fujii et al., 1988). After decapitation of the embryos, the hearts from one to five embryos were rapidly removed, trimmed of the atria and great vessels, and the ventricles (left and right) were cleaned of connective tissue and dissociated with brief, repeated exposures to collagenase and DNAase at 37°C as previous described (Brotto and Creazzo, 1996). The cultures were enriched for myocytes by 20-min incubations in tissue-culture flasks before plating the cells. During these short incubations other cell types attach to the flasks whereas myocytes do not. The myocytes were sparsely plated (~5×10^5 cells/35-mm culture dish) in DeHaan's 21212 medium with 1.8 mM $CaCl_2$, onto plastic petri dishes (Falcon, 1008, Becton Dickenson, San Jose, CA) containing a glass coverslip (25-mm diameter and 0.16-mm thickness). The cultures were incubated in a humidified 5% CO_2-95% air atmosphere at 37°C. The myocytes were cultured overnight and used within 24 h of enzymatic dissociation to allow for attachment to glass coverslips and to recover from the cell isolation procedure. EC coupling does not appear to be measurably affected by enzymatic dispersion and overnight culture. This is evident when comparing reports of SR contributions to electrically stimulated Ca^{2+} transients in isolated myocytes (Brotto and Creazzo, 1996; Creazzo et al., 1995) with Ca^{2+} transients elicited in freshly dissected intact cardiac trabeculae (Nosek et al., 1997), which shows that the Ca^{2+} transients from isolated myocytes are virtually identical to those obtained in intact trabeculae whether or not SR function is blocked with ryanodine. Moreover, a high level of colocalization of RyRs and DHPRs is maintained even after enzymatic dissociation and overnight culture in which the embryonic myocytes, unlike adult myocytes, have typically lost their elongated appearance and have assumed a spherical shape (Creazzo et al., 2001). Thus, junctional complexes are quite stable and not disrupted under the conditions used in this study. All experiments were carried out at room temperature (22–24°C).

Calcium transient measurements

Myocytes were loaded with fura-2 AM and calibrations were carried out as previously determined in our laboratory and described in detail elsewhere (Brotto and Creazzo, 1996). Within 24 h of cell isolation, the coverslips were transferred to a perfusion chamber (Warner Instruments, Hamden, CT), with maximum volume of 1 ml, and the cells were gently washed five times with a Ringer solution containing: 142.5 mM NaCl, 4.0 mM KCl, 1.8 mM $MgCl_2$, 1.8 mM $CaCl_2$, 5.0 mM HEPES (*n*-2-hydroxyethylpiperazine-*n*′-2-ethanesulfonic acid), and 10.0 mM dextrose, adjusted to pH 7.4 with NaOH, at room temperature. After washing the myocytes were incubated in 1 ml of Ringer solution with 1.5–2.0 μM fura-2 AM for 8 min at 37°C in a rotating water bath. The myocytes were subsequently washed five times with the Ringer solution without the dye and allowed to stand at room temperature for 30 min to facilitate the de-esterification of the dye and rinsed again before use. The chamber was subsequently placed on the stage of a Olympus IX-70 inverted microscope (Olympus America, Inc., Melville, NY). We have found that after exposure of myocytes loaded with fura-2 to saponin (a skinning agent that selectively permeabilizes the sarcolemmal membrane), the remaining fluorescence counts were not significantly different from the background autofluorescent counts before loading. These results indicate that subcellular compartmentalization of fura-2 is not detectable when using our standardized fura-2 AM loading conditions. A DeltaScan microspectrofluorometer with dual monochrometers (Photon Technology International, Inc., Lawrenceville, NJ) was used to collect the fura-2 calcium transients (340:380-nm ratios).

Electrical field stimulation

Electrical field stimulation at 0.2Hz was accomplished by applying 5 V for 5–7 ms via a pulse stimulator (Model II, Hewlett-Packard Co., Palo Alto, CA) through two platinum electrodes placed on either side of a single myocyte. The stimulator was triggered by a digital timer (Winston Electronics, San Francisco, CA).

Patch-clamp

The myocytes loaded with fura-2 were voltage-clamped, using the perforated patch-clamp technique as previously described (Brotto and Creazzo, 1996). Before use the culture medium was replaced with extracellular solution comprised of 1.8 mM $CaCl_2$, 20 mM CsCl, 120 mM TEA-Cl, 1.8 mM $MgCl_2$, 10 mM HEPES, 3 μM TTX ($\sim 500 \times K_I$ for the chick cardiac Na channel), and 5 mM dextrose, adjusted to pH 7.4 with NaOH. The perforated patch solution was comprised of 55 mM KCl, 70 mM Cs_2SO_4, 7 mM $MgCl_2$, 10 mM HEPES, and 5 mM dextrose (pH 7.3, KOH). Nystatin was added to this solution from a 50 mg/ml stock in DMSO (1:500 dilutions). The high concentrations of Cs and TEA were used to limit interference from K^+ currents.

For buffer power determinations Ca^{2+} transients were stimulated by activating Ca^{2+} current under voltage-clamp conditions by stepping to +10 mV from the holding potential of −80 mV. To block the SR contribution to the transient, SR Ca^{2+} release was inhibited with 100 μM ryanodine and SR Ca^{2+} uptake was blocked using 1 μM thapsigargin. It should be noted that computations involving the proportion of Ca^{2+} bound by the SR are subject to a potential error due to the use of thapsigargin in our experiments. Thapsigargin has been shown to reduce the Ca^{2+} binding affinity of the Ca^{2+}-ATPase in competition assays where the molar ratio of inhibitor to ATPase approaches 1 (Witcome et al., 1995). However, this effect should be limited under our experimental conditions because the concentration of SR Ca^{2+}-ATPase in the cytoplasm is much greater than the 1 μM thapsigargin used for the determination of Ca buffering. The molar ratios calculated from table 1 are 0.2:1, 0.08:1, and 0.06:1 for ED5, 11, and 15, respectively. Therefore, the error is expected to be small and probably not significant, particularly for ED11 and 15.

Estimation of accessible cell volume in chick ventricle

Computation of intracellular Ca^{2+} buffer power requires an estimate of the cell volume in which the fura-2 is dispersed, termed accessible cell volume (V_{acc}). V_{acc} is roughly the intracellular volume outside of mitochondria, which is ~65% of total cell volume in adult rat ventricular myocytes (Table 3 in Bers, 2001; Berlin et al., 1994). Similar values for extramitochondrial volume were obtained in adult avian heart (Table 3 in Bers, 2001). However, the volume of the sarcoplasmic reticulum (SR, 3.5% in rat ventricle; Bers, 2001) and that physically occupied by the concentrated protein in the cytosol (~10–15%; Bers, 2001) must also be considered, leaving a V_{acc} of ~47–52% for adult rat. Inasmuch as we were unaware of similar estimates in embryonic chick heart we devised a method to measure accessible cell volume in this tissue.

Small segments of embryonic left ventricle (8–12 mg wet weight) were dissected and split into strands connected centrally, like an octopus, to facilitate rapid diffusion into and out of the preparation. Dissection was performed at room temperature in oxygenated chick Ringer containing 30 mM BDM (2,3-butanedione 2-monoxime) to eliminate contractility and minimize cellular damage (Wiggins et al., 1980; Brotto et al., 1995). To estimate extracellular volume (V_{extra}), preparations were transferred to 0.5 ml of chick Ringer containing 0.024 μCi/μl-tritiated water (to label all cellular water) and 0.0024 μCi/μl of 14C-labeled mannitol (to label extracellular volume) for 30 min at 4°C. Samples were gently agitated to facilitate diffusion. The samples were then briefly blotted to remove excess fluid, placed in 5 ml of scintillation fluid, and gently agitated in a refrigerator for three days, after which the radioactivity was counted. The concentrations of tritiated water and 14C-mannitol and incubation times were determined by trial and error to give sufficient counts for accuracy. Along with the tissue samples, vials containing serial dilutions of tritiated water and 14C-mannitol were also counted, which established a linear relation to relate counts and marker concentrations.

The tissue volume outside of mitochondria, SR, and concentrated protein (V_{mito}) was estimated by bathing preparations for 30 min in a relaxing solution containing 0.45 mM Mg^{2+}, 2.59 mM MgATP, 15 mM disodium phosphocreatine, 5 mM EGTA, and 84.5 mM potassium methanesulfonate, at pH 7.1, with 5% v/v Dextran T-500 and 50 μg/ml saponin. Dextran minimizes swelling of the preparation (Godt and Maughan, 1981) and saponin at this concentration permeabilizes the sarcolemma but not the SR (Nosek et al., 1997). Preparations were subsequently treated as in the extracellular volume determinations above. The accessible cell volume (V_{acc}) necessary for our calculations is thus $V_{mito} - V_{extra}$.

As a test of the methodology, we treated other preparations for 30 min with 1% Triton X-100, a nonionic detergent, in chick relaxing solution with 5% Dextran to remove all membranes. The tissues were loaded with radiolabels and processed as outlined above. In this case, we expected the tritium space should be identical to that measured with mannitol.

Although ventricular tissue from ED5 was too fragile to withstand the blotting and transfer between solutions, successful estimates were obtained from ED11 and 15. At both ages, regression analysis showed that the ratio of tritium and mannitol spaces was not significantly different from 1.0, thus validating the method. Estimates of V_{extra} and V_{mito} for ED11 and 15 were not significantly different, so data were pooled to obtain values of V_{extra} of 5.7% (mean ± 0.1% SE, $n = 25$) and V_{mito} of 60.6% (mean ± 2.5% SE, $n = 26$). Taken together, these give an estimate of V_{acc} of 54.9% (mean ± 1.8% SE), a value in reasonable agreement with that of adult rat myocytes.

Cytoplasmic calibration of the fura-2

At the end of the experiment the myocyte was exposed to 10 μM of ionomycin (Ca salt) for the determination of the parameters R_{max} and β_{max}. The same cell was then exposed to 25 mM EGTA to determine R_{min} and β_{min}. In most cases the new ratio after exposure of the cell to either ionomycin or EGTA was achieved in 5–10 min. The myocyte autofluorescence was determined before loading with fura-2. Fura-2 transients were then calibrated in terms of $[Ca]_i$ with the ratiometric procedure used by Grynkiewicz et al. (1985) with the equation

$$[Ca]_i = K_d \times \beta \times (R - R_{min})/(R_{max} - R),$$

where K_D is the dissociation constant for fura-2 (224 nM); β is the ratio of the fluorescence signal at 380 nm of a solution with high Ca^{2+} (βmax) and low Ca^{2+} (βmin); R is the ratio at 340:380 nm; R_{min} is the ratio at 340:380 when the cell is in the presence of EGTA (low Ca^{2+}); and R_{max} is the ratio at 340:380 when the cell is in the presence of ionomycin (high Ca^{2+}). The K_D = 224 nM for fura-2 was taken from the estimate of Grynkiewicz et al. (1985) for a buffered high K^+, low Na^+, and Mg^{2+} solution.

Estimation of cytosolic fura-2 dye concentration

Dye concentration in myocytes is estimated by making fluorescence measurements of fura-2, of a known concentration, in an oil droplet submersed in a Ca^{2+}-free high K^+ solution as detailed by Moore et al. (1990) and as previously described (Brotto and Creazzo, 1996). Briefly, myocyte fura-2 concentration is calculated from

$$\begin{aligned} &Myocyte\,[fura\text{-}2] \\ &\quad = drop\,[fura\text{-}2] \times (drop\,V/myocyte\,V) \times \\ &\quad (myocyte\,counts/drop\,counts)/0.7, \end{aligned}$$

where V is volume and *counts* is photon counts at the isosbestic point. The counts are divided by 0.7, since light collection in oil is 70% as efficient as in water, as indicated by Moore and co-workers for a 40× objective.

Using our standardized loading conditions, $[fura\text{-}2]_i$ = 5.9 ± 2.4 μM (±SD; n = 23). The range varied from 3.3 to 10.9 μM $[fura\text{-}2]_i$. All measurements of cytosolic Ca buffering were corrected for Ca binding by fura-2 by assuming a K_D value of 224 μM.

Statistics

Statistical comparisons among the three embryonic ages were made using analysis of variance (ANOVA) for a single factor. Individual comparisons were made using either the student's *t*-test or the paired student's *t*-test when comparing paired data (i.e., before and after addition of ryanodine). $P < 0.05$ was considered significant. B_{max} and K_D were determined from experimental or theoretical data using Origin 6.1 software (OriginLab Corporation, Northampton, MA). Curve fitting was carried out using the nonlinear least-squares method and Origin 6.1 software.

RESULTS

For this study, embryonic ventricular myocytes were obtained from chick embryos at ED5, 11, and 15 and cultured overnight. The ages selected encompass nearly the full range of development for SR junctional complexes in the chick embryo, including the age when SR peripheral junctions are first detected to an age when the relative frequency of junctions is similar to an adult level (Protasi et al., 1996).

Ca^{2+} transients in ventricular development

The peak magnitude of Ca^{2+} transients, in the presence or absence of 100 μM ryanodine (to block SR Ca^{2+} release), was measured in field-stimulated ventricular myocytes at ED5, 11, and 15 (Fig. 1). Maximum reduction of the Ca^{2+} transient was achieved after a 20-min exposure to 100 μM ryanodine (Brotto and Creazzo, 1996). The magnitude of the transients was greatest at ED5 and declined with age. Most of the decline occurred between ED5 and 11 with the peak magnitude reduced by 33% over this time period. A further but much smaller decline occurred between ED11 and 15 (8.5%). Ryanodine (100 μM) reduced the magnitude by ~45% at ED11 and 15, compared with only 6% at ED5. The reduction with ryanodine shown for ED11 was similar to a previously reported observation from this laboratory for this age (Brotto and Creazzo, 1996). The time to reach peak magnitude after electrical stimulation was not significantly different for any of the ages either with or without ryanodine exposure (197 $\pm$ 11 ms, all groups combined; $p = 0.95$, ANOVA). However, the time for the transient to decay by half the peak magnitude was significantly faster at ED5 in comparison with either ED11 or 15 in the absence of ryanodine (332 $\pm$ 38, 477 $\pm$ 54, and 499 $\pm$ 63 ms for ED5, 11, and 15, respectively; $p = 0.02$ ANOVA) or in the presence of ryanodine (346 $\pm$ 20, 480 $\pm$ 39, and 512 $\pm$ 29 ms; $p = 0.001$). There was no significant difference in the decay times when comparing ED11 and 15 with or without ryanodine. The faster decay time at ED5 reflects the faster decay for the Ca^{2+} current at this age (see below). Ryanodine treatment did not significantly affect the decay times. These results most likely indicated that the Na^+/Ca^{2+} exchanger was sufficient to rapidly extrude Ca^{2+} in transients in which the magnitude had been reduced by the ryanodine. The diastolic Ca^{2+} level at each age was slightly decreased by the addition of ryanodine and this was more evident at the older ages. The results indicate that Ca^{2+}-induced Ca^{2+} release (CICR) from the SR is very limited at ED5 but increases substantially by ED11. The increase in CICR appears to level off between ED11 and 15, as there is little difference in the effect of ryanodine between these ages. Finally, the small effect of ryanodine on the magnitude of the Ca^{2+} transient at ED5 indicates that most of the transient at this age is due to an influx of extracellular Ca^{2+}.

Ca^{2+} current decreases with development

The results in Fig. 1 indicate that there is sparse SR function at ED5. A plausible explanation for the larger electrically stimulated Ca^{2+} transients at ED5 is that the voltage-gated Ca^{2+} current is larger at this age. To test this hypothesis, the magnitude of the Ca^{2+} current was measured in voltage-clamped myocytes (Fig. 2). Embryonic ventricular myocytes have both L-and T-type Ca^{2+} currents (Kawano and DeHaan, 1991; Brotto and Creazzo, 1996; Cribbs et al., 2001; Kitchens et al., 2003). The current-voltage (I-V) relationships in Fig. 2 *B* illustrate that the peak magnitudes of Ca^{2+} currents from ED5 to ED15 qualitatively parallels the decrease in the magnitude of the electrically stimulated Ca^{2+} transients during development. The holding potential for these experiments was -80 mV and both L- and T-type Ca^{2+} currents were activated with this voltage-clamp protocol (Kawano and DeHaan, 1991). This was evident in the biphasic appearance of the I-V relationships evident at ED11 and 15 (Fig. 2 *B*). At ED5 the I-V relationships for both currents overlapped more than at later ages, reflecting a more positive activation threshold for $I_{Ca,T}$ and a more negative activation for $I_{Ca,L}$ at earlier ages in the chick (Kawano and DeHaan, 1991). To examine in greater detail the decline of Ca^{2+} currents with development we relied on the voltage-dependent differences between L- and T-type current (Kawano and DeHaan, 1991; Brotto and Creazzo, 1996). To obtain the I-V relationship for L-type current, T-type current was inactivated by a 500-ms prepulse to -40 mV (Fig. 2 *C*). The T-type current I-V was calculated from the difference in the current elicited from -80 mV and that following the prepulse to -40 mV. The peak magnitude of T-type current occurred at ~–30 mV and L-type at 0 to +10 mV. The I-V relationship for T-type current at ED5 showed proportionately greater current at positive potentials. This may be due to differences in voltage-dependent properties observed at earlier embryonic ages (Kawano and DeHaan, 1991). These data indicated that both L- and T-type Ca^{2+} currents decline with development. Most of the decline in L-type current occurred between ED5 and 11, whereas T-type current appeared to decline steadily over the entire period from ED5 to 15. A similar developmental decline of L- and T-type currents was observed in an earlier study that employed a strategy of blocking L-type current with nifedipine when holding at -80 mV (Kitchens et al.,

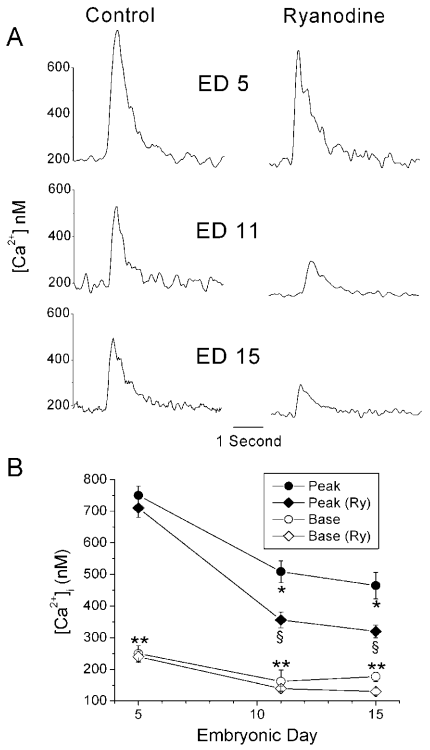

FIGURE 1 The effect of ryanodine (*Ry*) on electrically stimulated intracellular Ca^{2+} transients during development. (*A*) Examples of Ca^{2+} transients illustrating the effects before and after the addition of 100 μM ryanodine. Note that Ca^{2+} transients are larger at ED5 compared to ED11 and 15, whereas the effect of ryanodine is smaller. (*B*) Graphical representation illustrating that most of the decline in the magnitude of Ca^{2+} transients as well as the largest increase in the effect of ryanodine occurs between ED5 and 11. Peak indicates the peak magnitude of the Ca^{2+} transient and base indicates the baseline Ca^{2+} level after decay of the Ca^{2+} transient and just before the beginning of the next transient. $N = 7$ myocytes for each of the three ages. The data points represent 2–3 experiments per age with 2–4 myocytes per experiment. Error bars indicate mean ± SE. Single asterisk (*) indicates statistical significance when comparing either ED11 or 15 with ED5. Section symbol (§) indicates significant reduction in the peak after ryanodine treatment in paired comparisons with the student's *t*-test. Double asterisk (**) indicates that the baseline was significantly less after ryanodine treatment when compared using the paired student's *t*-test.

2003). These results indicate that the relatively large Ca^{2+} transients observed at ED5 were most likely due to a larger voltage-gated Ca^{2+} current although we cannot rule out a possible contribution from reverse Na^+/Ca^{2+} exchange.

From visual examination of the Ca^{2+} current records such as the examples in Fig. 2 *A* it appeared that the current decay was slower at ED11 and 15 compared to ED5. To verify this observation we fitted the decaying phase of the Ca^{2+} current with a single exponential curve. We used the current records from ~15 to 150 ms after the voltage step to −30 mV from the −80 mV holding potential for T-type current and after the voltage step to +10 mV following the prepulse to −40 mV for L-type current. These data were well fitted by a single exponential with no detectable improvement in the fit when fitted to a double-exponential curve (not shown). The exponential time constant for decay of the current at −30 mV was not significantly different among the three ages (combined $\tau = 24.5 \pm 1.7$ ms; $p = 0.74$, ANOVA). However at +10 mV, the decay times were significantly different ($\tau = 32.4 \pm 3.5$, 51.9 ± 4.6, and 54.4 ± 4.5 ms for ED5, 11, and 15, respectively; $p = 0.02$, ANOVA). As anticipated, the rate of decay at ED11 and 15 was significantly slower than at ED5 ($p < 0.01$ for both ages, Student's *t*-test). There was no difference between ED11 and 15 ($p = 0.41$). In summary, the rate of decay of L-type Ca^{2+} current is faster at ED5 than at the later ages.

SR Ca^{2+} content increases with development

The other major source of cytosolic Ca^{2+} for EC coupling is the SR. The Ca^{2+} content of the SR was estimated by releasing SR Ca^{2+} with a rapid application of a high concentration of caffeine (50 mM) and integrating the resultant Na^+/Ca^{2+} exchange current in voltage-clamped

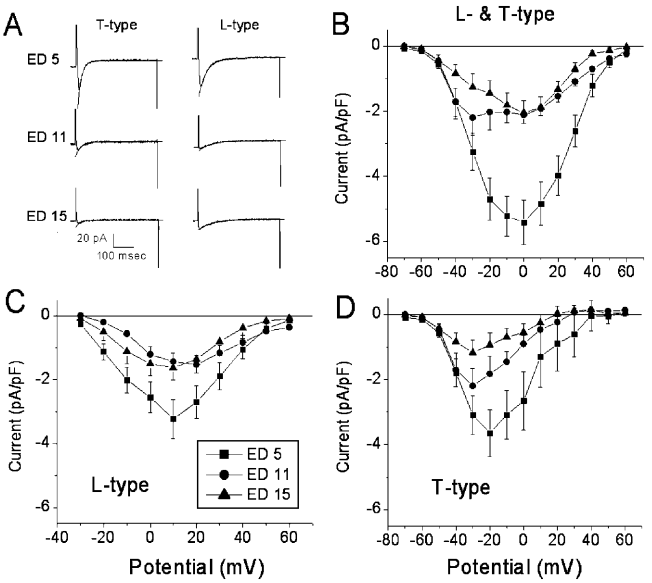

FIGURE 2 Examples of L- and T-type Ca^{2+} currents and current-voltage (I-V) relationships from ED5, 11, and 15. (*A*) Example of current traces illustrating T-type Ca^{2+} current elicited from steps to −30 mV from the holding potential of −80 mV and L-type current from a step to +10 mV after a prepulse to −40 mV to inactivate the T-current. Note that the Ca^{2+} currents are largest at ED5. The overlying smooth curves illustrate the single-exponential fits to the decaying phase of the currents. (*B*) I-V curves elicited by voltage steps from a −80-mV holding potential showing the peak values for inward Ca^{2+} currents. The biphasic I-V curve most noticeable at ED11 is due to the presence of T-type Ca^{2+} current which activates at a lower threshold compared to L-type current (see text). (*C*) I-V relationships for L-type Ca^{2+} current elicited after inactivation of T-type current with a 500-ms prepulse to −40 mV. (*D*) The I-V relationship for T-type current was determined by subtracting the values illustrated in *C* from those in *B*. $N = 15$, 10, and 15 for ED5, 11, and 15, respectively, and 3–5 cells per experiment. Error bars indicate mean ± SE.

myocytes (Diaz et al., 1996). As expected, the SR Ca^{2+} content increased markedly in a near-linear fashion with development (Fig. 3). These data are consistent with observations by others showing a developmental increase in SR Ca^{2+} release units and an accumulation of electron-dense material in SR vesicles (presumably calsequestrin) over a similar developmental period in chick heart (Protasi et al., 1996).

To assess the functional ability of the Na^+/Ca^{2+} exchanger to extrude Ca^{2+} with development, the rate of decay of the caffeine-induced transient was determined by exponential curve-fitting. The data were well-fitted by a single exponential (not shown) and were not significantly different among the three ages ($\tau = 77 \pm 16$, 102 ± 11, and 82 ± 5 ms for ED5, 11, and 15, respectively; $p = 0.20$, ANOVA). These results indicate that the exchanger density is not the rate-limiting step in the extrusion of Ca^{2+} in the absence of SR function.

Ca^{2+} buffer power during development

The approach of Berlin et al. (1994) was used to estimate the fast Ca^{2+} buffering active during the rapid rising phase of the Ca^{2+} transient. For these experiments, SR function was blocked by application of 1 μM thapsigargin (to prevent SR Ca^{2+} uptake) and 100 μM ryanodine (to block SR Ca^{2+} release) to the extracellular solution and Ca^{2+} currents were elicited by voltage-clamp steps to +10 mV from a holding potential of −80 mV which elicits both T- and L-type Ca^{2+} currents (see Fig. 2). In some instances the Ca^{2+} channel agonist Bay k 8644 was added to increase the size of the current and facilitate obtaining measurable transients. Examples of Ca^{2+} transients elicited under these voltage-clamp conditions from ED5 to ED15 are shown in Fig. 4. Data such as those shown in Fig. 4 were used to calculate the cytosolic buffer power (BP) following the method of Berlin et al. (1994; reviewed briefly here). To determine BP, the integrated Ca^{2+} current ($\int I_{Ca}$) was compared to the simultaneous change in free Ca^{2+}. The $\int I_{Ca}$ gives the total moles of Ca^{2+} entering the cytosol which must be converted into moles/liter to calculate BP. This is done using the cytosolic volume into which the Ca^{2+} is diluted (see Methods). The Michaelis-Menten relationship was used to compare free and bound Ca^{2+},

$$[BCa] = \frac{[Ca^{2+}] \times B_{max}}{K_D + [Ca^{2+}]}, \quad (1)$$

where B_{max} is the sum of the capacities of all cytosolic buffers, K_D is the lumped dissociation constant for all buffers, and $[BCa]$ is the concentration of bound Ca^{2+} calculated as total Ca^{2+} minus free Ca^{2+}. To compute fast Ca^{2+} BP where the change in free Ca^{2+} (d[Ca^{2+}]) parallels the change in bound Ca (d[BCa]), Eq. 1 can be differentiated with respect to Ca^{2+} such that

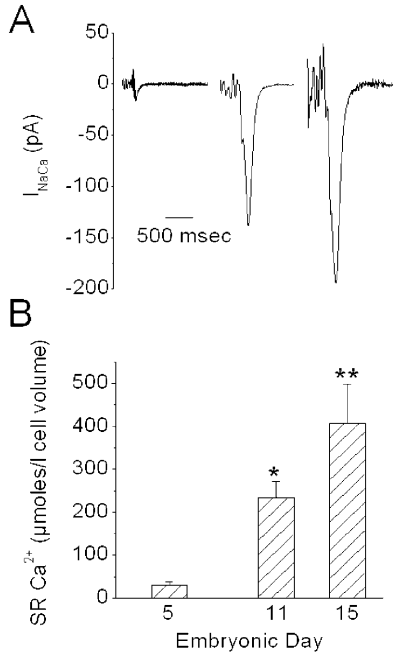

FIGURE 3 SR Ca^{2+} content determined from integration of the Na^+/Ca^{2+} exchange current after caffeine application. *A* shows an example of the exchanger current after caffeine application to a ventricular myocyte from ED5, 11, and 15 (*left to right*, respectively). The noisy baseline before the caffeine-induced current was due to the experimenter placing his hand and arm within the Faraday cage and close to the patch-amplifier head stage during the caffeine addition. The seal remained stable throughout this process. $N = 5$, 6, and 6, for ED5, 11, and 15, respectively, and representing two experiments per age and 2–3 cells per experiment. (*B*) Graphical representation of SR Ca^{2+} content. Single asterisk (*) indicates that ED11 SR content is significantly greater compared to ED5. Double asterisk (**) indicates significance when comparing ED15 with either ED5 or 11. Bars indicate mean ± SE.

$$\frac{d[BCa]}{d[Ca^{2+}]} = \frac{B_{max} \times K_D}{(K_D + [Ca^{2+}]_m)^2}, \quad (2)$$

where $[Ca^{2+}]_m$ is the mean level of Ca^{2+} during a step increase in Ca^{2+}. $[Ca^{2+}]_m$ was calculated by taking the difference between the Ca^{2+} level at the beginning of the depolarizing step to the peak value and dividing by 2. Fitting the data to Eq. 2 gives an estimate of B_{max} and K_D. Note that d[BCa]/d[Ca^{2+}] is the chord BP at any given cytosolic Ca^{2+} level. Fig. 5, *A–C*, show nonlinear fits of the data for the three experimental ages. The K_D was similar at all three developmental ages, whereas the B_{max} increased by 38% between ED5 and 15 with most of the increase occurring after ED11. These results can be compared to data from adult rat myocytes (Berlin et al., 1994), where estimated K_D was 0.96 μM and B_{max} was 123 μmol/liter cell H_2O.

Efficiency of CICR increases with development

The efficiency for SR CICR was expected to increase with development, with increasing SR Ca^{2+} content and de-

velopment of mature peripheral junctions. CICR efficiency was approximated by computing a simple gain factor for EC coupling. For this study, gain was approximated as

$$Gain = 1 + (SR\,Ca^{2+}\ release \div \int I_{Ca}/cell\ vol),$$

where $\int I_{Ca}/cell\ vol$ is the concentration of Ca^{2+} entering the cell via Ca^{2+} channels, referred to as the total accessible cell volume (55% of total cell volume; see Methods). Under this definition, gain is 1 if there is no contribution from the SR. Gain can be computed from the data with and without ryanodine shown in Fig. 1 *B*, since

$$SR\,Ca^{2+}\ release = Ca_{total} - Ca_{total\,(Ry)},$$

where Ca_{total} is the change in total Ca in the cytosol and is equal to the total Ca at the peak of the Ca^{2+} transient minus total Ca^{2+} at the base level. $Ca_{total\ (Ry)}$ is the total change in Ca in the cytosol in the presence of ryanodine and is equal to the total Ca in the presence of ryanodine at the peak minus that at the base in the presence of this drug. Total Ca at any free Ca^{2+} level is computed from Eq. 1 and the experimentally determined B_{max} and K_D at each age. The results for gain at the three experimental ages are shown in Fig. 6. As expected, gain increases with development as SR proliferates, and as peripheral couplings mature, with most of the increase occurring between ED5 and 11 ($gain$ = 1.05, 1.71, and 1.92, for ED5, 11, and 15, respectively). Another analogous way of expressing the efficiency of CICR is to compute the percent contribution of the SR to the total Ca^{2+} transient using the equation

$$\%\,SR\,Ca\ contribution = 100 \times SR\,Ca\ release \div (SR\,Ca\ release + \int I_{Ca}/cellvol).$$

Since SR Ca release is defined as $gain \times \int I_{Ca}/cell\ vol$,

$$\%\,SR\,Ca\ contribution = 100 \times (gain - 1) \div gain.$$

These data are also shown in Fig. 6.

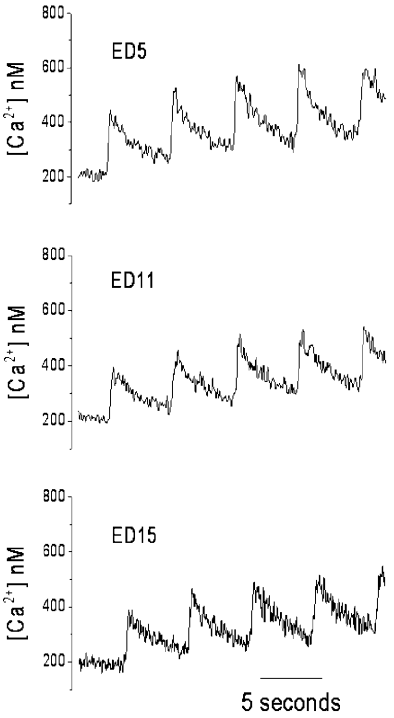

FIGURE 4 Example of Ca^{2+} transients used to calculate buffer power. SR function was blocked with 1 μM thapsigargin and 100 μM ryanodine. Shown are Ca^{2+} transients from five consecutive 200-ms voltage-clamp pulses to +10 mV from a holding potential of −80 mV at 5-s intervals. In some instances the Ca^{2+} channel agonist Bay k 8644 was added to increase the size of the Ca^{2+} current as in the examples for ED11 and 15 shown here. These data were used to calculate $[Ca^{2+}]_m$ as described in the text and illustrated in Fig. 5.

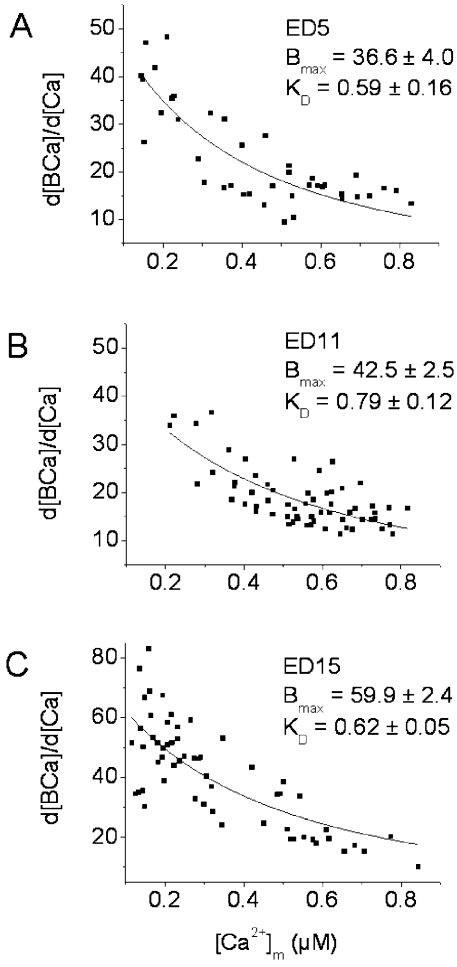

FIGURE 5 Cytosolic Ca buffering. $[Ca^{2+}]_m$ and d[BCa]/d[Ca] were calculated and fitted to Eq. 2 as described in the text. The K_D and B_{max} (mean ± SE) for each age are shown in *A–C*, and were determined by fitting the data set for each myocyte individually. The cumulative data for each age is shown in the graphs. Note that *d*[BCa]/*d*[Ca] is the chord buffer power for any given level of cytosolic-free Ca^{2+}. $N = 5$, 8, and 8, for ED5, 11, and 15, respectively. The data are from four experiments for each age and 1–3 cells per experiment. Units of B_{max} are in μM/liter cell water and K_D values are in μM.

Theoretical estimation of cytosolic BP

Cytosolic BP was calculated using K_D and B_{max} values of the major intracellular Ca^{2+} binding moieties given in Table 10 of Bers (2001) for adult rat cardiac myocytes, scaled appropriately for embryonic chick myocytes (Table 1). The major calcium binding moieties considered are TnC, SR Ca^{2+} pump, and low- and high-affinity binding to the sarcolemma (SL), as well as calmodulin, ATP, and PCr (creatine phosphate). The K_D and B_{max} values for these moieties are given in Table 1. Using these values, we generated the relationship between total bound Ca and free cytosolic Ca^{2+} over the range of 0.1 to 1 μM, which gave values of B_{max} and K_D for total cytosolic Ca buffering at the three embryonic ages. These values are displayed in Fig. 7 and are in reasonable agreement with experiment, especially given the uncertainties in the B_{max} and K_D of chick proteins.

Simulation of Ca^{2+} binding to these moieties using the on- and off-rates of binding demonstrate that peak binding occurred within a few ms of the peak of the Ca^{2+} transient (data not shown). The distribution of Ca among the major binding moieties at the peak of the Ca^{2+} transient at the three ages (from Fig. 1) is shown in Fig. 8. Note that, at all three ages, TnC is the major Ca binding moiety in the cytosol, and that the values for SR binding increase, as would be expected with SR proliferation with age. The relative increase in SR Ca binding is largely offset by declines in Ca bound by calmodulin and ATP.

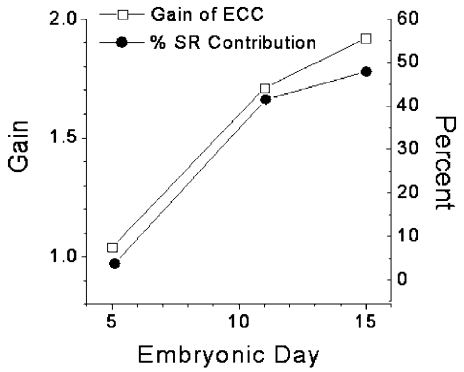

FIGURE 6 Computed gain factor for CICR and percent contribution to the Ca^{2+} transient from the SR are illustrated together for comparison. The values were calculated using the Ca^{2+} buffer power and the data from the field-stimulated Ca^{2+} transients illustrated in Fig. 1 as detailed in the text. The increase in gain and SR contribution parallels the structural development of SR junctions as demonstrated in Protasi et al. (1996; compare this Fig. 6 with their Fig. 4).

DISCUSSION

This is the first report providing a detailed analysis of variations in the Ca^{2+} handling properties of ventricular myocytes over an extended period of development. The findings indicate that the magnitude of electrically stimulated Ca^{2+} transients in embryonic ventricular myocytes declines by ~35% between ED5 and ED15 of development. The decline is due largely to a decline in the magnitude of

TABLE 1 Binding constants for major fast-acting Ca binding moieties

	ED15		ED11		ED5	
Embryonic day (ED)	B_{max} (μM)	K_D (μM)	B_{max} (μM)	K_D (μM)	B_{max} (μM)	K_D (μM)
TnC	33.6*	0.6†	28.7*	0.6†	20.3*	0.6†
SR	16‡	0.6	12‡	0.6	4‡	0.6
SL high§	0.25	0.3	0.25	0.3	0.25	0.3
SL low§	0.7	13	(Same all ages)			
Calmodulin total¶	24	0.1–1	(Same all ages)			
ATP‖	5000	200	(Same all ages)			
Creatine phosphate	12,000	71,073	(Same all ages)			

All values for K_D were taken from Table 10 in Bers (2001), except for those indicated by footnotes.

*Estimates of TnC in the embryonic chick heart were obtained from SDS PAGE gels of ventricular strips from ED5, 11, 15, and 24 days posthatching, run together on the same gel, using the larger and more prominent myosin band and assuming a 1:1 correspondence between myosin and TnC. B_{max} for TnC was assumed to be proportional to the myosin content normalized to total protein loading. We assumed that the TnC content at 24 days posthatching was the same as in adult rat myocytes, which Bers (2001) estimates is 70 μM.

†We have no accurate estimate of the K_D for TnC in embryonic chick myocytes and thus assume it is similar to adult rat myocytes (Bers, 2001).

‡To obtain an estimate of B_{max} for SR Ca^{2+} binding in embryonic chick heart we assumed 1), that the B_{max} was proportional to the oxalate-supported Ca^{2+} uptake in isolated chick SR reported by Vetter et al. (1986; their Fig. 2) and 2), that the B_{max} thus estimated from adult chicken SR uptake was the same as that in adult rat myocytes given in Bers (2001). B_{max} for ED5–15 were scaled proportionately from the adult value.

§Estimates of B_{max} for high- and low-affinity Ca^{2+} binding sites on SL were obtained using values for surface/volume ratio and the average volume of adult rat myocytes (Satoh et al., 1996). The chick myocytes used in this study were spherical with an average volume of ~3 pl. From geometry we obtained the surface area of chick myocytes. B_{max} for SL high- and low-affinity sites were scaled proportional to B_{max} of adult rat SL sites according to the relative surface area of chick and rat myocytes.

¶Calmodulin has four classes of calcium binding sites at which Mg and K also bind. Calcium binding to calmodulin was computed from binding affinities given in Fabiato (1983), assuming $[Mg^{2+}] = 0.6$ mM and $[K^+] = 140$ mM.

‖Calcium binding to ATP was computed from binding affinities for Ca, Mg, and K (Fabiato, 1983), given the values of $[Mg^{2+}]$ and $[K^+]$ above.

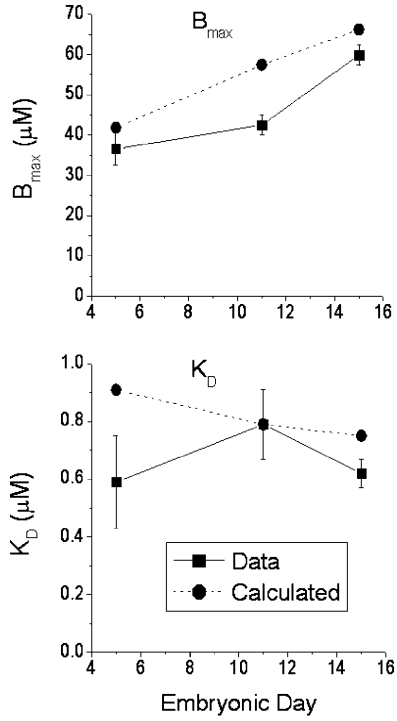

FIGURE 7 Measured data in comparison with theoretically calculated B_{max} and K_D values from estimates of the major fast Ca binding moieties in the cytoplasm. See text and Table 1.

voltage-gated Ca^{2+} current although the observed increase in the cytosolic buffering capacity would be expected to account for some of this decline. In contrast, the SR Ca^{2+} contribution to the Ca^{2+} transient increases markedly by nearly 12.5-fold over the same period of development, which corresponds to a 13.5-fold increase in the amount of Ca^{2+} stored by the SR. Important determinants of the free Ca^{2+} detected by fura-2 are the fast-acting Ca^{2+} buffers in the cytoplasm, which are expected to vary with development. The B_{max} for the fast Ca buffers increases by ~40% between ED5 and 15. These data indicate that the cytoplasmic chord buffer power for any given value of $[Ca^{2+}]_i$ increases with developmental age. Theoretical calculations indicate that this is due to increases in the B_{max} for both TnC and SR. Calculations utilizing buffer power measurements and the integral of the calcium current show that the gain factor for CICR increases ~20-fold between ED5 and 15.

Developmental decline in the magnitude of the Ca^{2+} transient

Most of the decline of electrically stimulated Ca^{2+} transients occurred between ED5 and 11, with a slight further decline by ED15. In the chick embryo the shapes of the action potentials differ only slightly between ED5 and 15, and probably have minimal, if any, measurable effect on the magnitude of electrically stimulated transients (see Sperelakis, 1982). Our

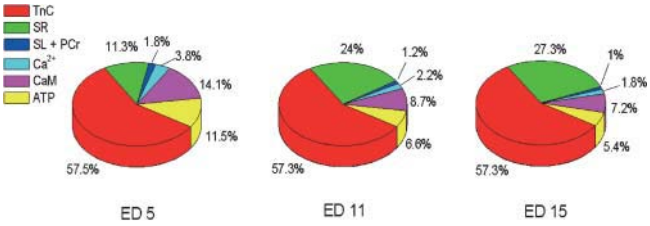

FIGURE 8 Graphical representation of the proportion of Ca^{2+} bound by the major cytoplasmic fast Ca^{2+} binding moieties at the peak of the intracellular Ca^{2+} transient at the three developmental ages. Note that TnC binds ~57% of the Ca^{2+} at each age. The proportion of Ca^{2+} bound by the SR increases, and this is offset primarily by corresponding decreases in Ca^{2+} bound by calmodulin and ATP. Ca^{2+} binding to total sarcolemmal (*SL*) sites and to creatine phosphate (*PCr*) is small and has been combined in the figure.

results indicate that the decline appears to be mostly due to a parallel decline in both L-and T-type Ca^{2+} currents. The decrease in the L-type Ca^{2+} current is not due to a decline in the number of L-type Ca^{2+} channels, as the number of DHP receptor binding sites is not significantly different throughout in-ovo development in the chick embryo (Marsh and Allen, 1989). One possible explanation is that the open channel probability for L-type channels decreases with development (Tohse et al., 1992) which may be related to the phosphorylation state of the channel. As of yet, the role of protein phosphorylation on Ca^{2+} channel activity in development has not been investigated. Another possibility is that there may be an embryonic form of the L-type channel that is not expressed in later development and that possesses different functional properties. This possibility is supported by a recent report of Ca^{2+} currents in embryonic mouse heart in a targeted knockout of α_{1C} by Seisenberger et al. (2000). The Seisenberger study provides convincing evidence for an as-yet unidentified L-type-like Ca^{2+} channel in the early developing heart that is later replaced by the cardiac α_{1C} isoform characteristic of adult myocardium.

Another observation of note is that the L-type Ca^{2+} current shows significantly faster inactivation at ED5 than at the later ages. The most likely explanation is that there is greater Ca^{2+}-dependent inactivation because of the relatively large Ca^{2+} current at this early age. A contributing factor may be the lower fast buffering capacity of the cytoplasm from less Ca^{2+} binding by SR and TnC. Recent evidence indicates that calmodulin, which appears to be tethered to the L-type channel, is thought to be a critical component of Ca^{2+}-dependent inactivation (reviewed in Bers, 2001). Although we assumed that the concentration of calmodulin remained constant during heart development, our calculations indicate that a higher proportion of entering Ca^{2+} is bound by calmodulin at ED5 than at ED11 or 15 (see Table 1 and Fig. 8). Taken together, these factors likely contribute to the fast inactivation even in the relative absence of local SR Ca^{2+} release, which is thought to contribute significantly to Ca^{2+}-dependent inactivation in adult heart (Puglisi et al., 1999).

Cytoplasmic Ca^{2+} buffering during development

The summed B_{max} for fast Ca^{2+} buffers increases with development. This is to be expected, inasmuch as the rate of cell division declines with development and the myocytes become more packed with myofibrils and the content of SR increases. The experimentally determined K_D and B_{max} values were in reasonable agreement with our theoretical predictions (see Fig. 7). We used these values in a unique approach to estimate the gain for CICR and the percent contribution from the SR in the global field-stimulated Ca^{2+} transients which increase with development.

Our theoretical estimations of Ca binding moieties indicates that TnC binds ~57% of entering Ca^{2+} during a transient at each of the three ages investigated. As expected, the proportion of Ca^{2+} bound by SR Ca^{2+}-ATPase increases with development, largely at the expense of that which is bound by ATP and calmodulin. The summed B_{max} for the fast Ca^{2+} buffers measured in the present study is approximately one-third that reported by Berlin et al. (1994). This appears to be largely due to ~50% lower B_{max} for TnC and ~70% lower value for SR binding compared to adult mammalian ventricle (compare our Table 1 with Table 10 in Bers, 2001).

In our approach to estimating cytosolic Ca^{2+} buffering, we used the global Ca^{2+} transient, which assumes that the transient was uniform throughout the myocyte. This is true for adult ventricular myocytes with an extensive t-tubular system regardless of whether SR function is blocked. A report by Haddock et al. (1999) on neonatal rabbit myocytes which lack t-tubules demonstrated with confocal line scans that the magnitude of the transient is greatest near the periphery and least toward the center of the myocyte. This nonuniform distribution of Ca^{2+} during a transient is likely to be similar in embryonic chick myocytes which have no t-tubules and no extended junctional SR. In this scenario, Ca^{2+} measurements restricted to the cell periphery are likely to lead to an underestimation of the cytosolic buffering capacity whereas central measurements will lead to an overestimation. Embryonic myocytes are spherical after enzymatic dissociation and this geometry should lead to an even distribution of the transient from periphery to center. Therefore, we assumed that regional differences in $[Ca^{2+}]_i$ are averaged-out in the global Ca^{2+} transient and, along with our detailed measurements of the assessable cell volume, we have obtained a good estimate of the total cytosolic Ca^{2+} buffering capacity.

Functional development of the SR

As expected, SR function as determined by the efficacy of ryanodine blockade of field-stimulated transients markedly increases between ED5 and 11 with a small increase thereafter (see Fig. 1). These data would suggest that most of the development of SR occurs between the ages of ED5 and 11. This hypothesis is supported by the report from Protasi, Franzini-Armstrong, and colleagues (Protasi et al., 1996), which shows a dramatic increase in the relative frequency of *complete junctions* that occur over the same period of development, and is consistent with our determinations of the gain factor for CICR and the proportion of transient due to SR Ca release (see Fig. 4 in Protasi et al., 1996, and compare with our Fig. 6). Complete junctions, defined on the basis of electron microscopic observations, are SR-plasma membrane junctional complexes in which the junctional gap is fully zippered by the closely spaced feet of the ryanodine receptor/Ca^{2+} release channel. There are virtually no complete junctions at ED5 but by ED11, nearly 80% of junctions are complete. Other measured parameters indicate that the length of junctional profiles with zippered feet and the number of peripheral couplings per unit length of plasma membrane are similar to adult by ED11. Moreover, the area of plasmalemmal junctional domains increases markedly between ED5 and 11, while not changing significantly between ED11 and 15. Together with the Protasi study, our data shows that the development of structure and function of SR junctions are well correlated.

The study by Protasi et al. (1996) suggests that the relatively low gain factor for SR CICR in ED5 myocytes is likely due to several factors including less SR, reduced SR Ca^{2+} stores from a lack of calsequestrin, and incomplete SR junctions lacking fully zippered arrays of RyRs. This conclusion is further supported by a recent study of EC coupling development in mouse embryonic stem cells by Sauer et al. (2001). These investigators found that the elementary SR Ca^{2+} release events (Ca^{2+} sparks) seen at an earlier stage of in vitro development were of lower frequency and magnitude than at a later stage, and attributed these observations to fewer RyRs and less Ca^{2+} load in the SR. These conclusions from the study of Sauer and co-workers are consistent with the SR morphology reported by Protasi and co-workers, and with our measurements of SR Ca^{2+} content and CICR gain factor in developing chick heart.

Species differences and EC coupling in embryonic versus adult heart

In mammals, it is usually considered that SR content is sparse at birth and undergoes most of its development postnatally (Nakanishi and Jarmakani, 1984). However, the level of maturity and function of the SR is species-dependent. For example, as mentioned in the Introduction, SR is sparse in rabbit and rat neonatal hearts (Seguchi et al., 1986b; Nakanishi et al., 1992) but not in guinea pigs, which have a fully developed SR at birth (Goldstein and Traeger, 1985). Moreover, during a Ca^{2+} transient, Ca^{2+} removal from the cytoplasm is dependent more on extrusion into the extracellular space via the Na^+/Ca^{2+} exchanger in neonatal rabbit, whereas the SR Ca^{2+}-ATPase plays a larger role in neonatal rat (Bassani and Bassani, 2002; Balaguru et al.,

1997). By contrast, SR morphology and function in the chick is well developed by hatching (Protasi et al., 1996). In agreement, our results indicate that CICR from the SR parallels the morphological development, in that CICR is well developed by ED15 in the chick (see Discussion above).

Regardless of the species, in early embryonic heart development the SR is likely to be very sparse or entirely absent. This implies a simplified EC coupling, in which all of the Ca^{2+} contributing to the Ca^{2+} transient is derived from the extracellular space via voltage-gated Ca^{2+} channels and possible entry from reverse-mode Na^+/Ca^{2+} exchange and extrusion of Ca^{2+} via the exchanger working in its normal forward mode. However, EC coupling in the early heart tube has not been investigated, and there may be other contributing factors unique to early development. In working with a targeted knockout of the cardiac Na^+/Ca^{2+} exchanger (NCX1), we observed relatively normal Ca^{2+} transients in heart tubes from 9.5 days postcoitum mouse embryos (Koushik et al., 2001). This intriguing finding suggests the possibility of other potent mechanisms for the extrusion of Ca^{2+} in early heart development.

A common feature of embryonic and early neonatal or posthatching ventricular myocytes is the absence of t-tubules, and SR junctional complexes are all at the periphery of the cell, producing spatial-temporal characteristics of the global Ca^{2+} transient different from that of adult (discussed above; Haddock et al., 1999). In this feature and along with smaller size, these myocytes resemble atrial and nodal pacemaking cells. Within a week of postnatal development mammalian ventricular myocytes begin to develop an extensive t-tubular system, although in avian species there are no t-tubules, but an extensive system of extrajunctional SR that develops instead (Sommer, 1995). A major advantage in the use of the avian embryo is that because of its early maturity, SR CICR can be studied without the complicating influences of t-tubules and extrajunctional or corbular SR.

A second but less studied common feature of immature ventricle is the presence of significant T-type Ca^{2+} current as demonstrated in the chick embryo in this report and also in embryonic mouse (Cribbs et al., 2001). T-type currents are absent in adult ventricle and are confined largely to atrial and nodal cells and Purkinje fibers, and are thought to be important for cardiac autorhythmicity. We recently reported that Ca^{2+} entry via T-type channels contributes significantly to the global Ca^{2+} transient and can stimulate CICR after nifedipine block of L-type channels (Kitchens et al., 2003). More work is needed to clearly establish the function of this important ion channel in the developing myocardium.

SUMMARY AND CONCLUSIONS

To our knowledge, this is the first report to quantify in detail the maturation of cardiac EC coupling and Ca^{2+} handling over an extended period of development. We made direct measurements of the Ca buffering capacity of the cytoplasm and used these data in a unique approach to estimate the gain factor for CICR and the contribution of the SR to the global Ca^{2+} transient. Not surprisingly, these factors increase markedly with development and moreover, the increases occur in a manner consistent with detailed published data on the structural development of SR peripheral junctions. We have provided estimates of the changes in the contributions of the major fast Ca binding moieties over an extended period of development. Finally, at all ages examined, TnC binds at least half of the entering Ca^{2+} during a transient and as expected, the proportion bound by the SR increases.

From the data presented here and the above discussion it is apparent that all of the primary structural components necessary for a relatively mature level of EC coupling are present by ED11. Does this mean that the efficiency or, in other words, the gain factor for CICR, develops in synchrony with the appearance of the primary components for cardiac EC coupling? The results from this report indicate that this is the case, and thus it appears that the development of structure and function of SR junctions are well correlated.

We thank Ms. Jane Chu for her careful determinations of the accessible cell volume, and for SDS PAGE of ventricular strips.

This work was supported by National Institutes of Health grants HL58861, HL36059, and HL71015.

REFERENCES

Balaguru, D., P. S. Haddock, J. L. Puglisi, D. M. Bers, W. A. Coetzee, and M. Artman. 1997. Role of the sarcoplasmic reticulum in contraction and relaxation of immature rabbit ventricular myocytes. *J. Mol. Cell. Cardiol.* 29:2747–2757.

Bassani, R. A., and J. W. M. Bassani. 2002. Contribution of Ca^{2+} transporters to relaxation in intact ventricular myocytes from developing rats. *Am. J. Physiol. Heart Circ. Physiol.* 282:H2406–H2413.

Berlin, J. R., J. W. M. Bassani, and D. M. Bers. 1994. Intrinsic cytosolic calcium buffering properties of single rat cardiac myocytes. *Biophys. J.* 67:1775–1787.

Bers, D. M. 2001. Excitation-Contraction Coupling and Cardiac Contractile Force, 2nd ed. Kluwer Academic Publishers, Boston, MA.

Brotto, M. A. D., and T. L. Creazzo. 1996. Ca^{2+} transients in embryonic chick heart: contributions from Ca^{2+} channels and the sarcoplasmic reticulum. *Am. J. Physiol. Heart Circ. Physiol.* 270:H518–H525.

Brotto, M. A. P., R. T. H. Fogaça, T. L. Creazzo, R. E. Godt, and T. M. Nosek. 1995. The effect of 2,3-butanedione 2-monoxime (BDM) on ventricular trabeculae from the avian heart. *J. Muscle Res. Cell Motil.* 16:1–10.

Creazzo, T. L., M. A. P. Brotto, and J. Burch. 1995. Reduced Ca^{2+} transients and Ca^{2+} currents during early and late cardiac dysmorphogenesis. *FASEB J.* 9:A557.

Creazzo, T. L., R. E. Godt, L. Leatherbury, S. J. Conway, and M. L. Kirby. 1998. Role of cardiac neural crest cells in cardiovascular development. *Annu. Rev. Physiol.* 60:267–286.

Creazzo, T. L., Q. Wang, and R. E. Godt. 2001. Colocalization of dihydropyridine and ryanodine receptors in developing heart with a neural crest-associated defect. *Exp. Cardiol.* 6:11–16.

Cribbs, L. L., B. L. Martin, E. A. Schroder, B. B. Keller, B. P. Delisle, and J. Satin. 2001. Identification of the T-type calcium channel ($Ca_V3.1d$) in developing mouse heart. *Circ. Res.* 88:403–407.

Diaz, M. E., S. J. Cook, J. P. Chamunorwa, A. W. Trafford, M. K. Lancaster, S. C. O'Neill, and D. A. Eisner. 1996. Variability of spontaneous Ca^{2+} release between different rat ventricular myocytes is correlated with Na^{+}-Ca^{2+} exchange and $[Na^{+}]_i$. *Circ. Res.* 78:857–862.

Dutro, S. M., J. A. Airey, C. F. Beck, J. L. Sutko, and W. R. Trumble. 1993. Ryanodine receptor expression in embryonic avian cardiac muscle. *Dev. Biol.* 155:431–441.

Fujii, S., R. K. Ayer, Jr., and R. L. DeHaan. 1988. Development of the fast sodium current in early embryonic chick heart cells. *J. Membr. Biol.* 101:209–223.

Fabiato, A. 1983. Calcium-induced release from the cardiac sarcoplasmic reticulum. *Am. J. Physiol.* 245:C1–14.

Godt, R. E., R. T. H. Fogaça, and T. M. Nosek. 1991. Changes in force and calcium sensitivity in the developing avian heart. *Can. J. Physiol. Pharmacol.* 69:1692–1697.

Godt, R. E., and D. W. Maughan. 1981. Influence of osmotic compression on calcium activation and tension in skinned muscle fibers of the rabbit. *Pflüegers Arch.* 391:334–337.

Goldstein, M. A., and L. Traeger. 1985. Ultrastructural changes in postnatal development of the cardiac myocyte. *In* The Developing Heart. M. L. Legato, editor. Martinus Nijhoff, Boston, MA. 1–20.

Grynkiewicz, G., M. Poenie, and R. Y. Tsien. 1985. A new generation of calcium indicators with greatly improved fluorescence properties. *J. Biol. Chem.* 260:3440–3450.

Haddock, P. S., W. A. Coetzee, E. Cho, L. Porter, H. Katoh, D. M. Bers, M. S. Jafri, and M. Artman. 1999. Subcellular $[Ca^{2+}]_i$ gradients during excitation-contraction coupling in newborn rabbit ventricular myocytes. *Circ. Res.* 85:415–427.

Jewett, P. H., S. D. Leonard, and J. R. Sommer. 1973. Chicken cardiac muscle. *J. Cell Biol.* 56:595–600.

Junker, J., J. R. Sommer, M. Sar, and G. Meissner. 1994. Extended junctional sarcoplasmic reticulum of avian cardiac muscle contains functional ryanodine receptors. *J. Biol. Chem.* 269:1627–1634.

Kawano, S., and R. L. DeHaan. 1991. Developmental changes in the calcium currents in embryonic chick ventricular myocytes. *J. Membr. Biol.* 120:17–28.

Kitchens, S. A., J. Burch, and T. L. Creazzo. 2003. T-type Ca^{2+} current contribution to Ca^{2+}-induced Ca^{2+} release in developing myocardium. *J. Mol. Cell. Cardiol.* 35:515–523.

Koushik, S. V., J. Wang, R. Rogers, D. Moskophidis, N. A. Lambert, T. L. Creazzo, and S. J. Conway. 2001. Targeted inactivation of the sodium-calcium exchanger (*Ncx1*) results in the lack of a heartbeat and abnormal myofibrillar organization. *FASEB J.* 15:1209–1211.

Manasek, F. J. 1970. Histogenesis of the embryonic myocardium. *Am. J. Cardiol.* 25:149–168.

Marsh, J. D., and P. D. Allen. 1989. Developmental regulation of cardiac calcium channels and contractile sensitivity to $[Ca]_o$. *Am. J. Physiol. Heart Circ. Physiol.* 256:H179–H185.

Moore, E. D. W., P. L. Becker, K. E. Fogarty, D. A. Williams, and F. S. Fay. 1990. Ca^{2+} imaging in single living cells: theoretical and practical issues. *Cell Calcium.* 11:157–179.

Nakanishi, T., and J. M. Jarmakani. 1984. Developmental changes in myocardial mechanical function and subcellular organelles. *Am. J. Physiol. Heart Circ. Physiol.* 246:H615–H625.

Nakanishi, T., M. Seguchi, and A. Takao. 1992. Developmental changes in myocardial mechanical function and subcellular organelles. *Experientia.* 44:936–944.

Nosek, T. M., R. T. Fogaca, C. J. Hatcher, M. A. Brotto, and R. E. Godt. 1997. Effect of cardiac neural crest ablation on contractile force and calcium uptake and release in chick heart. *Am. J. Physiol. Heart Circ. Physiol.* 273:H1464–H1471.

Protasi, F., X. H. Sun, and C. Franzini-Armstrong. 1996. Formation and maturation of the calcium release apparatus in developing and adult avian myocardium. *Dev. Biol.* 173:265–278.

Puglisi, J. L., W. L. Yuan, J. W. M. Bassani, and D. M. Bers. 1999. Ca^{2+} influx through Ca^{2+} channels in rabbit ventricular myocytes during action potential clamp: influence of temperature. *Circ. Res.* 85:E7–E16.

Satoh, H., L. M. D. Delbridge, L. A. Blatter, and D. M. Bers. 1996. Surface:volume relationship in cardiac myocytes studied with confocal microscopy and membrane capacitence measurements: species dependence and developmental effects. *Biophys. J.* 70:1494–1504.

Sauer, H., T. Theben, J. R. Hescheler, M. Lindner, M. C. Brandt, and M. Wartenberg. 2001. Characteristics of calcium sparks in cardiomyocytes derived from embryonic stem cells. *Am. J. Physiol. Heart Circ. Physiol.* 281:H411–H421.

Seguchi, M., J. Harding, and J. Jamrmakani. 1986a. Developmental change in the function of sarcoplasmic reticulum. *J. Mol. Cell. Cardiol.* 18:189–195.

Seguchi, M., J. M. Jarmakani, B. L. George, and J. Harding. 1986b. Effect of Ca^{2+} antagonists on mechanical function in the neonatal heart. *Pediatr. Res.* 20:838–842.

Seisenberger, C., V. Specht, A. Welling, J. Platzer, A. Pfeifer, S. Kühbandner, J. Striessnig, N. Klugbauer, R. Feil, and F. Hofmann. 2000. Functional embryonic cardiomyocytes after disruption of the L-type α_{1C} ($Ca_v1.2$) calcium channel gene in the mouse. *J. Biol. Chem.* 275:39193–39199.

Sommer, J. R. 1995. Comparative anatomy: in praise of a powerful approach to elucidate mechanisms translating cardiac excitation into purposeful contraction. *J. Mol. Cell. Cardiol.* 27:19–35.

Sperelakis, N. 1982. Pacemaker mechanisms in myocardial cells during development of embryonic chick heart. *In* Cardiac Rate and Rhythm. L. N. Bouman and H. J. Jongsna, editors. Martinus Nijhoff, Dordrecht, The Netherlands. 129–65.

Sun, X.-H., F. Protasi, M. Takahashi, H. Takeshima, D. G. Ferguson, and C. Franzini-Armstrong. 1995. Molecular architecture of membranes involved in excitation-contraction coupling of cardiac muscle. *J. Cell Biol.* 129:659–671.

Tohse, N., J. Mészáros, and N. Sperelakis. 1992. Developmental changes in long-opening behavior of L-type Ca^{2+} channels in embryonic chick heart cells. *Circ. Res.* 71:376–384.

Vetter, R., H. Will, I. Kuttner, C. Kemsies, and L. Will-Shahab. 1986. Developmental changes of Ca transport systems in chick heart. *Biomed. Biochim. Acta.* 45:219–222.

Wiggins, G. R., J. Reiser, D. F. Fitzpatrick, and J. L. Bergey. 1980. Inotropic actions of diacetyl monoxime in cat ventricle muscle. *J. Pharmacol. Exp. Ther.* 212:217–224.

Witcome, M., Y. M. Khan, J. M. East, and A. G. Lee. 1995. Binding of sesquiterpene lactone inhibitors to the Ca^{2+}-ATPase. *Biochem. J.* 310:859–868.